



Time-dependent reliability analysis model under fuzzy state and its safety lifetime model

Yingshi Hu¹ · Zhenzhou Lu¹ · Jingyu Lei¹

Received: 17 April 2019 / Revised: 27 May 2019 / Accepted: 25 June 2019 / Published online: 27 July 2019
© Springer-Verlag GmbH Germany, part of Springer Nature 2019

Abstract

In view of the lack of time-dependent reliability analysis model (TDRA) under fuzzy state, which is ubiquitous in engineering, a TDRA model under fuzzy state is proposed in this paper, followed by the corresponding safety lifetime model. To establish the TDRA model under fuzzy state, this paper firstly transforms the TDRA model under binary state into a form expressed by the time-dependent failure domain indicator function, and then the TDRA model under fuzzy state is derived based on the basic principle of the time-independent reliability analysis (TIRA) model under fuzzy state. By introducing an auxiliary variable and establishing the time-dependent generalized performance function, the TDRA model under fuzzy state is transformed into a generalized one under binary state, where the failure domain and safety domain are clearly defined. Then, the single-loop Kriging (SLK) surrogate model approach is used to efficiently estimate the time-dependent failure probability (TDFP) in the special service time interval under fuzzy state. Based on the generalized TDRA model and its efficient estimation, a safety lifetime model constrained by the target TDFP under fuzzy state and a corresponding efficient solving method are presented. Finally, examples are used to verify the rationality of the TDRA model and the safety lifetime model under fuzzy state established in this paper, and the efficiency of the algorithm is also validated.

Keywords Fuzzy state · Time-dependent reliability analysis model · Safety lifetime model

1 Introduction

Due to the influence of external environment and self-aging, the structural performance will decrease with the increase of service time, and then the reliability level will decrease. The safety lifetime of the structure is the longest service time under the condition that the reliability of the structure is bigger than the target value (Fan et al. 2018). In the traditional time-independent reliability analysis (TIRA), it is generally considered that the loads on the structure and the performance of the structure will not change with the time (Sahinidis 2004). However, the loads usually change with service time, and the performance of the structure will also change with time because of the factors such as corrosion and fatigue (Hu et al. 2013; Yu et al. 2018; Yun et al. 2016). For this type of

problem, we need a time-dependent reliability analysis (TDRA) model (Wang et al. 2018b; Wang et al. 2019) to measure the reliability level.

TDRA often takes more computational cost than TIRA. The proposed TDRA methods can be divided into three categories, i.e., the crossing rate-based method (Andrieu-Renaud et al. 2004; Hu and Du 2013; Shi et al. 2017b), the extreme value-based method (Li et al. 2007; Shi et al. 2017a; Shi et al. 2018b; Yu and Wang 2018), and the surrogate model method (Feng et al. 2019; Hu and Mahadevan 2016; Wang and Wang 2015). The crossing rate-based method firstly assumes that the crossing of the performance function from the safety domain to the failure domain at any time in a given time interval obeys a specific distribution (such as Poisson distribution) and the crossings are independent with each other (Andrieu-Renaud et al. 2004). Thus, the time-dependent failure probability (TDFP) can be rewritten into the form of the integral of the crossing rate in the time interval of interest. The main drawback of this method is that the accuracy decreases if there exists multiple dependent crossings during the time interval of interest (Du 2014). The extreme value-based method only focuses on the extreme value of the output in a given time interval. By the extreme value transformation, the time-

Responsible Editor: Pingfeng Wang

✉ Zhenzhou Lu
zhenzhoulu@nwpu.edu.cn

¹ School of Aeronautics, Northwestern Polytechnical University, Xi'an 710072, People's Republic of China

dependent problem can be transformed into the time-independent one (Shi et al. 2017a), which can be analyzed by efficient TIRA methods, i.e., approximately analytical method, Monte Carlo Simulation (MCS) method and time-independent surrogate model method. The approximately analytical method uses the moments of the output expressed by the performance function to estimate the failure probability (Baran et al. 2012; Shi et al. 2018a). The MCS method is widely applicable but time-consuming, and the various advanced MCS methods were proposed to reduce the computational cost, such as importance sampling method (Au 2004; Au and Beck 1999; Grooteman 2008), subset simulation method (Au and Beck 2001; Song et al. 2009), line sampling method (Schuëller et al. 2004; Song and Lu 2007), and directional sampling method (Ditlevsen et al. 1990). The time-independent surrogate model method estimates the failure probability by constructing a cheap surrogate model replacing the original performance function to reduce the computational cost (Cheng and Lu 2018a, b; Echard et al. 2011; Yang et al. 2019). The extreme value method can greatly reduce the cost of computation, but it should be noted that the extreme value cannot be easily solved in engineering application. The surrogate model method performs the TDRA by constructing the surrogate model of the actual performance function; thereby the number of calling the actual model will be greatly reduced. At present, the most commonly used surrogate model methods for TDRA include the double-loop Kriging model (Wang and Wang 2015) and the single-loop Kriging (SLK) model (Hu and Mahadevan 2016; Yun et al. 2016). The double-loop Kriging model is proposed on the idea of the extreme value-based method. The inner loop establishes the Kriging surrogate model of the time-dependent performance function with respect to the time at a given realization of the random input vector. By using the inner Kriging surrogate model to obtain the extreme value in the time interval of interest at the training sample approximately, the outer loop establishes the Kriging surrogate model of the extreme value with respect to the random input vector for estimating the TDFP. The SLK model performs reliability analysis by directly constructing the Kriging surrogate model for the original time-dependent performance function with respect to the random inputs and the time. Compared with the double-loop Kriging model, the SLK sufficiently considers the relationship between random input vector and time, thus the SLK model is more efficient than the double-loop one.

The methods introduced above are based on the assumption of binary state, i.e., there is a clear boundary between the failure state and the safety state of the structure. However, in practical engineering, there exists universally a gradual failure mode due to thermal creep or fatigue cracks caused by alternating loads, where the boundary between failure state and safety state is fuzzy (Tang and Lu 2014). In view of the TIRA problem under fuzzy state,

Cai (Cai et al. 1991a, b, 1993) and Onisawa (Onisawa 1990) established a Profust reliability analysis model under probability inputs and fuzzy state described by a given membership function. In Profust reliability analysis model, the failure probability can be defined as the expectation of the membership function of the performance function to the fuzzy failure state. Many scholars have researched the estimation method of Profust model; the basic method to estimate Profust model is the MCS method. When the sample size approaches infinity, the result of MCS converges to the true value, but this method requires a large amount of computation cost to obtain a convergent result because it is based on the law of large numbers. In order to improve the computational efficiency, Chen (Chen and Lu 2007) employed the line sampling method under binary state to estimate the Profust model. Feng (Feng et al. 2018) combined the subset simulation method to reduce the computational cost of MCS for estimating the Profust model. Wang (Wang et al. 2018a) reduced the computational cost by converting the integral domain. However, the existing reliability methods for Profust model are only applicable to time-independent problems, and there still lacks TDRA model under fuzzy state. But, the fuzzy state exists widely in the time-dependent structural systems; therefore, it is necessary to establish a TDRA model under fuzzy state.

The main contribution of this paper is establishing a TDRA model under fuzzy state by referring to the TIRA model under fuzzy state. To establish the TDRA model under fuzzy state, the TDRA model under binary state is transformed firstly. The TDFP under binary state is expressed by the form of the time-dependent failure domain indicator function so that the TDRA model under fuzzy state can be conveniently established by the basic principle of TIRA model under fuzzy state. On the established TDRA model under fuzzy state, the auxiliary variable and time-dependent generalized performance function are introduced to simplify the TDRA model under fuzzy state. Then, the safety lifetime model is constructed by the constraints of target TDFP under fuzzy state, and the SLK surrogate model method is introduced to solve the TDFP and the safety lifetime.

In this paper, the method of establishing the TDRA model under fuzzy state is given in Sect. 2, and the derivation process and the corresponding solution method of time-dependent generalized performance function are included. The safety lifetime model based on the time-dependent generalized performance function is constructed in Sect. 3, and the corresponding solution method is also provided. Section 4 gives the example analysis to validate the reasonability of the TDRA model under fuzzy state and the efficiency of the corresponding safety lifetime solution. The conclusions of this paper are drawn in Sect. 5.

2 TDRA model under fuzzy state and solving method

In this section, the TIRA model under fuzzy state is reviewed, on which the TDRA model under fuzzy state is established. The algorithm for solving the TDFP under fuzzy state is also provided in this section.

2.1 TIRA model

Based on the definition of the TIRA model under binary state and that under fuzzy state, the corresponding relationship between the two models is analyzed in Sect. 2.1. Then, according to the existing literature (Wang et al. 2018a), the TIRA model under fuzzy state is transformed into that under binary state (where the failure domain is clearly separated from the safety domain) by introducing an auxiliary variable. By virtue of the TIRA model under fuzzy state and its transformed form, the TDRA model under fuzzy state and its generalized form are established in Sect. 2.2, on which Sect. 2.3 provides the solution for the TDFP under fuzzy state.

2.1.1 TIRA model under binary state

The indicator function $I_F(\cdot)$ of the failure domain $F = \{\mathbf{x} : g(\mathbf{x}) \leq 0\}$ and the indicator function $I_S(\cdot)$ of the safety domain $S = \{\mathbf{x} : g(\mathbf{x}) > 0\}$ in the TIRA model under binary state possess the following relationship:

$$I_F(g(\mathbf{x})) = 1 - I_S(g(\mathbf{x})) \tag{1}$$

where $g(\mathbf{x})$ is the time-independent performance function and $\mathbf{x} = \{x_1, x_2, \dots, x_n\}$ is a realization of the n -dimensional random input vector $\mathbf{X} = \{X_1, X_2, \dots, X_n\}$.

The failure domain is defined as $F = \{\mathbf{x} : g(\mathbf{x}) \leq 0\}$. $I_F(g(\mathbf{x})) = 1$ if $\mathbf{x} \in F$, and $I_F(g(\mathbf{x})) = 0$ otherwise. The safety domain is defined as $S = \{\mathbf{x} : g(\mathbf{x}) > 0\}$. $I_S(g(\mathbf{x})) = 1$ if $\mathbf{x} \in S$, and $I_S(g(\mathbf{x})) = 0$ otherwise. Figure 1 shows the relationship of $I_F(g(\mathbf{x}))$ and $I_S(g(\mathbf{x}))$ vs $g(\mathbf{x})$. The

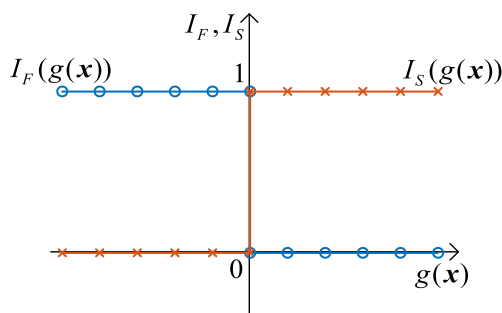


Fig. 1 The relationship of $I_F(g(\mathbf{x}))$ and $I_S(g(\mathbf{x}))$ vs $g(\mathbf{x})$

corresponding failure probability P_f has the following relationship with the reliability P_r ,

$$P_f = \int_{-\infty}^{+\infty} I_F(g(\mathbf{x})) f_X(\mathbf{x}) d\mathbf{x} \tag{2}$$

$$P_r = \int_{-\infty}^{+\infty} I_S(g(\mathbf{x})) f_X(\mathbf{x}) d\mathbf{x} \tag{3}$$

$$= \int_{-\infty}^{+\infty} (1 - I_F(g(\mathbf{x}))) f_X(\mathbf{x}) d\mathbf{x} = 1 - P_f$$

2.1.2 TIRA model under fuzzy state

Under the condition of fuzzy state, the membership function $\mu_{\tilde{F}}(g(\mathbf{x}))$ of $g(\mathbf{x})$ to the fuzzy failure domain \tilde{F} and the membership function $\mu_{\tilde{S}}(g(\mathbf{x}))$ of $g(\mathbf{x})$ to the fuzzy safety domain \tilde{S} have the following relationship.

$$\mu_{\tilde{F}}(g(\mathbf{x})) = 1 - \mu_{\tilde{S}}(g(\mathbf{x})) \tag{4}$$

$\mu_{\tilde{F}}(g(\mathbf{x}))$ is a non-increasing function of $g(\mathbf{x})$ and $\mu_{\tilde{S}}(g(\mathbf{x}))$ is a non-decreasing function of $g(\mathbf{x})$ generally. Figure 2 shows the schematic diagram of $\mu_{\tilde{F}}(g(\mathbf{x}))$ and $\mu_{\tilde{S}}(g(\mathbf{x}))$ vs $g(\mathbf{x})$. The relationship between the failure probability \tilde{P}_f and the reliability \tilde{P}_r under fuzzy state is the same as that under binary state, and it is shown as follows:

$$\tilde{P}_f = \int_{-\infty}^{+\infty} \mu_{\tilde{F}}(g(\mathbf{x})) f_X(\mathbf{x}) d\mathbf{x} \tag{5}$$

$$\tilde{P}_r = \int_{-\infty}^{+\infty} \mu_{\tilde{S}}(g(\mathbf{x})) f_X(\mathbf{x}) d\mathbf{x} \tag{6}$$

$$= \int_{-\infty}^{+\infty} (1 - \mu_{\tilde{F}}(g(\mathbf{x}))) f_X(\mathbf{x}) d\mathbf{x} = 1 - \tilde{P}_f$$

Comparing Eqs. (2) and (5), it can be found that after considering the fuzziness of the failure state, the failure probability model is transformed from the expectation of the indicator function of the failure domain under binary state to that of the membership function of the failure domain under fuzzy state. A similar connection can also be found by comparing Eqs. (3) and (6). Section 2.2 will

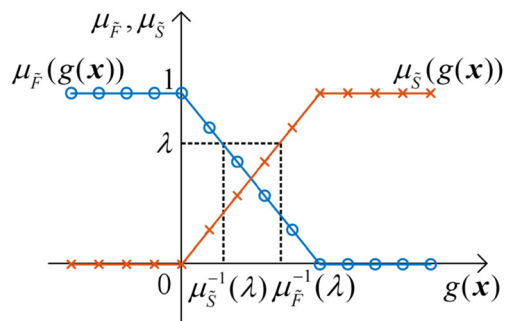


Fig. 2 The relationship of $\mu_{\tilde{F}}(g(\mathbf{x}))$ and $\mu_{\tilde{S}}(g(\mathbf{x}))$ vs $g(\mathbf{x})$

use this corresponding relationship to establish a TDRA model under fuzzy state.

2.1.3 TIRA model under fuzzy state and its generalized form under binary state

According to the proof in literature (Wang et al. 2018a), Eqs. (5) and (6) can be rewritten into the following forms,

$$\tilde{P}_f = \int_{-\infty}^{+\infty} \mu_{\tilde{F}}(g(\mathbf{x})) f_X(\mathbf{x}) d\mathbf{x} = \int_0^1 \text{Prob}\{g(\mathbf{x}) \leq \mu_{\tilde{F}}^{-1}(\lambda)\} d\lambda \quad (7)$$

$$\tilde{P}_r = \int_{-\infty}^{+\infty} \mu_{\tilde{S}}(g(\mathbf{x})) f_X(\mathbf{x}) d\mathbf{x} = \int_0^1 \text{Prob}\{g(\mathbf{x}) > \mu_{\tilde{F}}^{-1}(\lambda)\} d\lambda \quad (8)$$

in which $\lambda \in [0, 1]$ is the corresponding membership degree of $g(\mathbf{x})$, $\mu_{\tilde{F}}^{-1}(\cdot)$ is the inverse function of the fuzzy failure domain membership function, $\text{Prob}\{\cdot\}$ is the probability operator.

Because $\text{Prob}\{g(\mathbf{x}) \leq \mu_{\tilde{F}}^{-1}(\lambda)\} + \text{Prob}\{g(\mathbf{x}) > \mu_{\tilde{F}}^{-1}(\lambda)\} = 1$, $\tilde{P}_f + \tilde{P}_r = 1$ still holds, which shows that \tilde{P}_f and \tilde{P}_r satisfy the property of self-duality. Define the clear domain defined by the inequality $g(\mathbf{x}) \leq \mu_{\tilde{F}}^{-1}(\lambda)$ as the generalized clear failure domain F_λ , then F_λ can be expressed as follows:

$$F_\lambda = \{\mathbf{x} : g(\mathbf{x}) \leq \mu_{\tilde{F}}^{-1}(\lambda)\} \quad (9)$$

Introduce a standard normal random variable $X_{n+1} \sim N(0, 1)$ independent with \mathbf{X} , and let $\lambda = \Phi(x_{n+1})$ ($\Phi(\cdot)$ is the cumulative distribution function of the standard normal variable), and substitute it into Eq. (7). Then, the conversion expression of the failure probability under fuzzy state can be obtained as follows:

$$\begin{aligned} \tilde{P}_f &= \int_{-\infty}^{+\infty} \text{Prob}\{g(\mathbf{x}) \leq \mu_{\tilde{F}}^{-1}(\Phi(x_{n+1}))\} d\Phi(x_{n+1}) \\ &= \int_{-\infty}^{+\infty} \text{Prob}\{g(\mathbf{x}) \leq \mu_{\tilde{F}}^{-1}(\Phi(x_{n+1}))\} \phi(x_{n+1}) dx_{n+1} \quad (10) \\ &= \int_{g(\mathbf{x}) \leq \mu_{\tilde{F}}^{-1}(\Phi(x_{n+1}))} f_X(\mathbf{x}) \phi(x_{n+1}) d\mathbf{x} dx_{n+1} \end{aligned}$$

where $\phi(\cdot)$ is the probability density function (PDF) of the standard normal variable.

Equation (10) is a time-independent failure probability under binary state with the generalized clear failure domain $\{\mathbf{x} : g(\mathbf{x}) - \mu_{\tilde{F}}^{-1}(\Phi(x_{n+1})) \leq 0\}$. Compared with the original problem, the time-independent failure probability under fuzzy state is transformed into that under binary state with the generalized clear failure domain $\{\mathbf{x} : g(\mathbf{x}) - \mu_{\tilde{F}}^{-1}(\Phi(x_{n+1})) \leq 0\}$

by introducing a standard normal variable X_{n+1} independent with \mathbf{X} . Similarly, the reliability under fuzzy state can also be converted by the following Eq. (11).

$$\begin{aligned} \tilde{P}_r &= \int_{-\infty}^{+\infty} \text{Prob}\{g(\mathbf{x}) > \mu_{\tilde{F}}^{-1}(\Phi(x_{n+1}))\} d\Phi(x_{n+1}) \\ &= \int_{-\infty}^{+\infty} \text{Prob}\{g(\mathbf{x}) > \mu_{\tilde{F}}^{-1}(\Phi(x_{n+1}))\} \phi(x_{n+1}) dx_{n+1} \quad (11) \\ &= \int_{g(\mathbf{x}) > \mu_{\tilde{F}}^{-1}(\Phi(x_{n+1}))} f_X(\mathbf{x}) \phi(x_{n+1}) d\mathbf{x} dx_{n+1} \end{aligned}$$

Equations (10) and (11) completely convert the time-independent failure probability \tilde{P}_f and reliability \tilde{P}_r under fuzzy state into those under binary state with the generalized clear failure domain $\{\mathbf{x} : g(\mathbf{x}) - \mu_{\tilde{F}}^{-1}(\Phi(x_{n+1})) \leq 0\}$ and the generalized clear safety domain $\{\mathbf{x} : g(\mathbf{x}) - \mu_{\tilde{F}}^{-1}(\Phi(x_{n+1})) > 0\}$, respectively. Therefore, many existing reliability analysis methods developed under binary state can be used to estimate the reliability under fuzzy state.

2.2 TDRA model

This section constructs the TDRA model under fuzzy state based on the concept of constructing the TIRA model under fuzzy state in Sect. 2.1. For employing the principle and the derivation of TIRA model under fuzzy state to establish the TDRA model under fuzzy state, the TDRA model under binary state is firstly transformed as the expectation of the time-dependent failure domain indicator. Then, the expression of the TDRA model under binary state is consistent with that of the TIRA model under binary state, on which the basic principle of the TIRA model under fuzzy state can be conveniently used to establish the TDRA model under fuzzy state. On the other hand, the TDRA model expressed by the expectation of the time-dependent failure domain indicator can also be validated by the equivalent TIRA model obtained by the extreme value of the TDRA model. To simplify the established TDRA model under fuzzy state, an auxiliary variable is introduced so that the existing solving methods for the TDRA model under binary state can be directly employed to solve the established TDRA model under fuzzy state.

2.2.1 TDRA model under binary state

The time-dependent performance function $y = g(\mathbf{x}, t)$ changes with time in the time interval $t \in [t_0, t_e]$ of interest generally. When the TDRA model is established from the perspective of the time-dependent failure domain and safety domain under binary state, the time-dependent failure domain $F(t_0, t_e)$ and

the time-dependent safety domain $S(t_0, t_e)$ can be expressed by Eqs. (12) and (13), and Fig. 3 gives the relationship of the time-dependent failure domain $F(t_0, t_e)$ in the time interval $[t_0, t_e]$ with the failure domain $F(t, t) = \{\mathbf{x} : g(\mathbf{x}, t) \leq 0\}$ at instant t ($t \in [t_0, t_e]$) for a more intuitive understanding of the time-dependent failure domain.

$$\begin{aligned}
 F(t_0, t_e) &= \{\mathbf{x} : g(\mathbf{x}, t) \leq 0, \exists t \in [t_0, t_e]\} \\
 &= \left\{ \mathbf{x} : \min_{t \in [t_0, t_e]} g(\mathbf{x}, t) \leq 0 \right\} = \{\mathbf{x} : g(\mathbf{x}, t^*) \leq 0\} \quad (12) \\
 S(t_0, t_e) &= \{\mathbf{x} : g(\mathbf{x}, t) > 0, \forall t \in [t_0, t_e]\} \\
 &= \left\{ \mathbf{x} : \min_{t \in [t_0, t_e]} g(\mathbf{x}, t) > 0 \right\} \\
 &= \{\mathbf{x} : g(\mathbf{x}, t^*) > 0\} \quad (13)
 \end{aligned}$$

where $t^* = \arg \min_{t \in [t_0, t_e]} g(\mathbf{x}, t)$.

Then, the corresponding TDFP $P_f(t_0, t_e)$ and time-dependent reliability $P_r(t_0, t_e)$ can be obtained as follows:

$$\begin{aligned}
 P_f(t_0, t_e) &= \text{Prob}\{F(t_0, t_e)\} = \text{Prob}\left\{ \mathbf{x} : \min_{t \in [t_0, t_e]} g(\mathbf{x}, t) \leq 0 \right\} \\
 &= \int_{\min_{t \in [t_0, t_e]} g(\mathbf{x}, t) \leq 0} f_X(\mathbf{x}) d\mathbf{x} \quad (14)
 \end{aligned}$$

$$\begin{aligned}
 P_r(t_0, t_e) &= \text{Prob}\{S(t_0, t_e)\} = \text{Prob}\left\{ \mathbf{x} : \min_{t \in [t_0, t_e]} g(\mathbf{x}, t) > 0 \right\} \\
 &= \int_{\min_{t \in [t_0, t_e]} g(\mathbf{x}, t) > 0} f_X(\mathbf{x}) d\mathbf{x} \quad (15)
 \end{aligned}$$

Obviously, we have $P_f(t_0, t_e) + P_r(t_0, t_e) = 1$, which satisfies the property of self-duality. By virtue of the construction of the TIRA model under fuzzy state, in order to use the TDRA

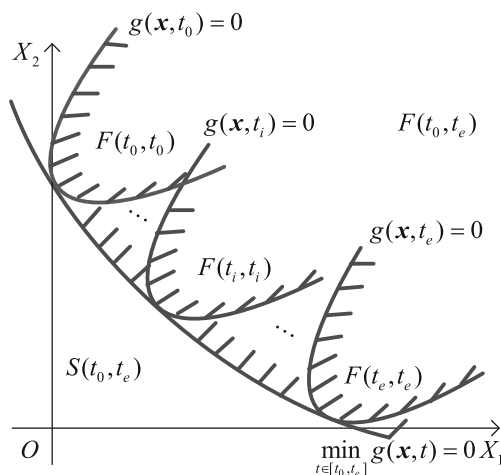


Fig. 3 The relationship of $F(t_0, t_e)$ with $F(t, t)$

model under binary state to construct the TDRA model under fuzzy state, the TDRA model under binary state should be rewritten from the perspective of the failure domain indicator function and the safety domain indicator function firstly.

The failure domain $F(t, t) = \{\mathbf{x} : g(\mathbf{x}, t) \leq 0\}$ indicator function $I_{F(t, t)}(g(\mathbf{x}, t))$ at instant t in the time-dependent problem has the following relationship with the safety domain $S(t, t) = \{\mathbf{x} : g(\mathbf{x}, t) > 0\}$ indicator function $I_{S(t, t)}(g(\mathbf{x}, t))$ at instant t ,

$$I_{F(t, t)}(g(\mathbf{x}, t)) = 1 - I_{S(t, t)}(g(\mathbf{x}, t)) \quad (16)$$

in which $I_{F(t, t)}(g(\mathbf{x}, t)) = \begin{cases} 1 & g(\mathbf{x}, t) \leq 0 \\ 0 & g(\mathbf{x}, t) > 0 \end{cases}$, $I_{S(t, t)}(g(\mathbf{x}, t)) = \begin{cases} 1 & g(\mathbf{x}, t) > 0 \\ 0 & g(\mathbf{x}, t) \leq 0 \end{cases}$. Generally, $I_{F(t, t)}(g)$ is a non-increasing function of g , and $I_{S(t, t)}(g)$ is a non-decreasing function of g .

For time-dependent failure domain $F(t_0, t_e) = \{\mathbf{x} : g(\mathbf{x}, t) \leq 0, \exists t \in [t_0, t_e]\}$ and time-dependent safety domain $S(t_0, t_e) = \{\mathbf{x} : g(\mathbf{x}, t) > 0, \forall t \in [t_0, t_e]\}$, their indicator functions $I_{F(t_0, t_e)}(g(\mathbf{x}, t))$ and $I_{S(t_0, t_e)}(g(\mathbf{x}, t))$ are respectively shown as follows:

$$I_{F(t_0, t_e)}(g(\mathbf{x}, t)) = \max_{t \in [t_0, t_e]} I_{F(t, t)}(g(\mathbf{x}, t)) \quad (17)$$

$$I_{S(t_0, t_e)}(g(\mathbf{x}, t)) = \min_{t \in [t_0, t_e]} I_{S(t, t)}(g(\mathbf{x}, t)) \quad (18)$$

in which $I_{F(t, t)}(g(\mathbf{x}, t)) = \begin{cases} 1 & g(\mathbf{x}, t) \leq 0 \\ 0 & g(\mathbf{x}, t) > 0 \end{cases}$, $I_{S(t, t)}(g(\mathbf{x}, t)) = \begin{cases} 1 & g(\mathbf{x}, t) > 0 \\ 0 & g(\mathbf{x}, t) \leq 0 \end{cases}$.

Since $I_{F(t, t)}(g(\mathbf{x}, t))$ is a non-increasing function of $g(\mathbf{x}, t)$ and $I_{S(t, t)}(g(\mathbf{x}, t))$ is a non-decreasing function of $g(\mathbf{x}, t)$, Eqs. (17) and (18) can be rewritten as

$$I_{F(t_0, t_e)}(g(\mathbf{x}, t)) = I_{F(t, t)}\left(\min_{t \in [t_0, t_e]} g(\mathbf{x}, t)\right) = I_{F(t^*, t^*)}(g(\mathbf{x}, t^*)) \quad (19)$$

$$I_{S(t_0, t_e)}(g(\mathbf{x}, t)) = I_{S(t, t)}\left(\min_{t \in [t_0, t_e]} g(\mathbf{x}, t)\right) = I_{S(t^*, t^*)}(g(\mathbf{x}, t^*)) \quad (20)$$

where $t^* = \arg \min_{t \in [t_0, t_e]} g(\mathbf{x}, t)$.

According to the above formula and from the perspective of the time-dependent failure domain indicator function $I_{F(t_0, t_e)}(g(\mathbf{x}, t))$, the TDFP under binary state can be established as follows:

$$\begin{aligned}
 P_f(t_0, t_e) &= \int_{-\infty}^{+\infty} I_{F(t_0, t_e)}(g(\mathbf{x}, t)) f_X(\mathbf{x}) d\mathbf{x} \\
 &= \int_{-\infty}^{+\infty} \max_{t \in [t_0, t_e]} I_{F(t, t)}(g(\mathbf{x}, t)) f_X(\mathbf{x}) d\mathbf{x} \\
 &= \int_{-\infty}^{+\infty} I_{F(t, t)}\left(\min_{t \in [t_0, t_e]} g(\mathbf{x}, t)\right) f_X(\mathbf{x}) d\mathbf{x} \\
 &= \int_{\min_{t \in [t_0, t_e]} g(\mathbf{x}, t) \leq 0} f_X(\mathbf{x}) d\mathbf{x} \quad (21)
 \end{aligned}$$

Comparing Eqs. (14) and (21), it can be seen that the TDFP under binary state established from the conversion of extreme value (Eq. (14)) and that from the conversion of time-dependent failure domain indicator function (Eq. (21)) have the same form. Similarly, the time-dependent reliability model shown as follows can be estimated from the perspective of the time-dependent safety domain indicator function.

$$\begin{aligned}
 P_r(t_0, t_e) &= \int_{-\infty}^{+\infty} I_{S(t_0, t_e)}(g(\mathbf{x}, t)) f_X(\mathbf{x}) d\mathbf{x} \\
 &= \int_{-\infty}^{+\infty} \min_{t \in [t_0, t_e]} I_{S(t, t)}(g(\mathbf{x}, t)) f_X(\mathbf{x}) d\mathbf{x} \\
 &= \int_{-\infty}^{+\infty} I_{S(t, t)} \left(\min_{t \in [t_0, t_e]} g(\mathbf{x}, t) \right) f_X(\mathbf{x}) d\mathbf{x} \\
 &= \int \min_{t \in [t_0, t_e]} g(\mathbf{x}, t) > 0 f_X(\mathbf{x}) d\mathbf{x} \tag{22}
 \end{aligned}$$

2.2.2 TDFP model under fuzzy state

Comparing the time-independent failure probability model under binary state shown in Eq. (2) with that under fuzzy state shown in Eq. (5), and combining with the TDFP model established from the perspective of the time-dependent failure domain indicator function $I_{F(t_0, t_e)}(\cdot)$ shown in Eq. (21), we can establish the TDFP $\tilde{P}_f(t_0, t_e)$ model under fuzzy state in the following Eq. (23):

$$\tilde{P}_f(t_0, t_e) = \int_{-\infty}^{+\infty} \mu_{\tilde{F}(t, t)} \left(\min_{t \in [t_0, t_e]} g(\mathbf{x}, t) \right) f_X(\mathbf{x}) d\mathbf{x} \tag{23}$$

in which the fuzzy failure domain $\tilde{F}(t, t)$ membership function $\mu_{\tilde{F}(t, t)}(\cdot)$ and the fuzzy safety domain $\tilde{S}(t, t)$ membership function $\mu_{\tilde{S}(t, t)}(\cdot)$ have the following relationship under the instant t :

$$\mu_{\tilde{F}(t, t)}(g(\mathbf{x}, t)) = 1 - \mu_{\tilde{S}(t, t)}(g(\mathbf{x}, t)) \tag{24}$$

Note that $\mu_{\tilde{F}(t, t)}(g(\mathbf{x}, t))$ is a non-increasing function of $g(\mathbf{x}, t)$ and $\mu_{\tilde{S}(t, t)}(g(\mathbf{x}, t))$ is a non-decreasing function of $g(\mathbf{x}, t)$.

Let $t^* = \arg \min_{t \in [t_0, t_e]} g(\mathbf{x}, t)$, then Eq. (23) can be rewritten as the following form:

$$\begin{aligned}
 \tilde{P}_f(t_0, t_e) &= \int_{-\infty}^{+\infty} \mu_{\tilde{F}(t, t)} \left(\min_{t \in [t_0, t_e]} g(\mathbf{x}, t) \right) f_X(\mathbf{x}) d\mathbf{x} \\
 &= \int_{-\infty}^{+\infty} \mu_{\tilde{F}(t^*, t^*)} (g(\mathbf{x}, t^*)) f_X(\mathbf{x}) d\mathbf{x} \tag{25}
 \end{aligned}$$

Equation (25) completely transforms the TDFP under fuzzy state into a time-independent failure probability under fuzzy state with the performance function of

$g(\mathbf{x}, t^*) = \min_{t \in [t_0, t_e]} g(\mathbf{x}, t)$. Therefore, Eq. (25) can be transformed into the following form with reference to Eq. (7).

$$\begin{aligned}
 \tilde{P}_f(t_0, t_e) &= \int_{-\infty}^{+\infty} \mu_{\tilde{F}(t^*, t^*)} (g(\mathbf{x}, t^*)) f_X(\mathbf{x}) d\mathbf{x} \\
 &= \int_0^1 \text{Prob} \left\{ g(\mathbf{x}, t^*) \leq \mu_{\tilde{F}(t^*, t^*)}^{-1}(\lambda) \right\} d\lambda \tag{26}
 \end{aligned}$$

Similarly, introduce $X_{n+1} \sim N(0, 1)$ which is independent with \mathbf{X} , and let $\lambda = \Phi(x_{n+1})$. Then, substitute $\lambda = \Phi(x_{n+1})$ and $d\lambda = \phi(x_{n+1}) dx_{n+1}$ into Eq. (26), we have Eq. (27) as follows:

$$\begin{aligned}
 \tilde{P}_f(t_0, t_e) &= \int_0^1 \text{Prob} \left\{ g(\mathbf{x}, t^*) \leq \mu_{\tilde{F}(t^*, t^*)}^{-1}(\lambda) \right\} d\lambda \\
 &= \int_{-\infty}^{+\infty} \text{Prob} \left\{ g(\mathbf{x}, t^*) \leq \mu_{\tilde{F}(t^*, t^*)}^{-1}(\Phi(x_{n+1})) \right\} \phi(x_{n+1}) dx_{n+1} \\
 &= \int_{g(\mathbf{x}, t^*) \leq \mu_{\tilde{F}(t^*, t^*)}^{-1}(\Phi(x_{n+1}))} f_X(\mathbf{x}) \phi(x_{n+1}) dx dx_{n+1} \tag{27}
 \end{aligned}$$

The above formula transforms the TDFP under fuzzy state into the failure probability with the time-independent clear failure domain $F^e = \left\{ (\mathbf{x}, x_{n+1}) : g(\mathbf{x}, t^*) \leq \mu_{\tilde{F}(t^*, t^*)}^{-1}(\Phi(x_{n+1})) \right\}$. The time-independent generalized performance function $g^e(\mathbf{x}, x_{n+1})$ corresponding to F^e is defined as follows:

$$g^e(\mathbf{x}, x_{n+1}) = g(\mathbf{x}, t^*) - \mu_{\tilde{F}(t^*, t^*)}^{-1}(\Phi(x_{n+1})) \tag{28}$$

In general, $\mu_{\tilde{F}(t, t)}(g)$ does not change with time, and only this case is considered in this paper. Then, the equivalent time-independent generalized performance function shown in Eq. (28) can be rewritten as

$$g^e(\mathbf{x}, x_{n+1}) = g(\mathbf{x}, t^*) - \mu_{\tilde{F}(t_0, t_0)}^{-1}(\Phi(x_{n+1})) \tag{29}$$

And, the equivalent time-independent clear failure domain F^e can be rewritten as follows.

$$F^e = \left\{ (\mathbf{x}, x_{n+1}) : g(\mathbf{x}, t^*) - \mu_{\tilde{F}(t_0, t_0)}^{-1}(\Phi(x_{n+1})) \leq 0 \right\} \tag{30}$$

Then, the TDFP $\tilde{P}_f(t_0, t_e)$ under fuzzy state can be transformed as the time-independent failure probability with the time-independent generalized performance function $g^e(\mathbf{x}, x_{n+1})$.

$$\begin{aligned}
 \tilde{P}_f(t_0, t_e) &= \int_{F^e} f_X(\mathbf{x}) \phi(x_{n+1}) dx dx_{n+1} \\
 &= \int_{g^e(\mathbf{x}, x_{n+1}) \leq 0} f_X(\mathbf{x}) \phi(x_{n+1}) dx dx_{n+1} \tag{31}
 \end{aligned}$$

Similarly, the time-dependent reliability model under fuzzy state can be established in Sect. 2.2.3 as follows.

2.2.3 Time-dependent reliability model under fuzzy state

Comparing the time-independent reliability model under binary state shown in Eq. (3) with that under fuzzy state shown

in Eq. (6), and combining with the time-dependent reliability model established from the perspective of the time-dependent safety domain indicator function $I_{S(t_0,t_e)}(\cdot)$ shown in Eq. (22), we can establish the time-dependent reliability $\tilde{P}_r(t_0, t_e)$ model under fuzzy state in the following Eq. (32):

$$\tilde{P}_r(t_0, t_e) = \int_{-\infty}^{+\infty} \mu_{\tilde{S}}(t, t) \left(\min_{t \in [t_0, t_e]} g(\mathbf{x}, t) \right) f_X(\mathbf{x}) dx \tag{32}$$

Similarly, let $t^* = \arg \min_{t \in [t_0, t_e]} g(\mathbf{x}, t)$, Eq. (32) can be rewritten as follows:

$$\begin{aligned} \tilde{P}_r(t_0, t_e) &= \int_{-\infty}^{+\infty} \mu_{\tilde{S}}(t, t) \left(\min_{t \in [t_0, t_e]} g(\mathbf{x}, t) \right) f_X(\mathbf{x}) dx \\ &= \int_{-\infty}^{+\infty} \mu_{\tilde{S}}(t^*, t^*) (g(\mathbf{x}, t^*)) f_X(\mathbf{x}) dx \end{aligned} \tag{33}$$

Obviously, the above formula completely transforms the time-dependent reliability under fuzzy state into a time-independent one with the performance function $g(\mathbf{x}, t^*) = \min_{t \in [t_0, t_e]} g(\mathbf{x}, t)$. Refer to the transformation formula of time-independent reliability under fuzzy state in Eq. (8), and Eq. (33) can be written as follows:

$$\begin{aligned} \tilde{P}_r(t_0, t_e) &= \int_{-\infty}^{+\infty} \mu_{\tilde{S}}(t^*, t^*) (g(\mathbf{x}, t^*)) f_X(\mathbf{x}) dx \\ &= \int_0^1 \text{Prob} \{ g(\mathbf{x}, t^*) > \mu_{\tilde{F}}^{-1}(t^*, t^*) (\lambda) \} d\lambda \end{aligned} \tag{34}$$

Similarly, introduce $X_{n+1} \sim \mathcal{N}(0, 1)$ independent with \mathbf{X} , and let $\lambda = \Phi(x_{n+1})$. Then substitute $\lambda = \Phi(x_{n+1})$ and $d\lambda = \phi(x_{n+1}) dx_{n+1}$ into Eq. (34), considering $\mu_{\tilde{F}}(t, t)(g) = \mu_{\tilde{F}}(t_0, t_0)(g)$; meanwhile, Eq. (35) can be derived as follows:

$$\begin{aligned} \tilde{P}_r(t_0, t_e) &= \int_0^1 \text{Prob} \{ g(\mathbf{x}, t^*) > \mu_{\tilde{F}}^{-1}(t_0, t_0) (\lambda) \} d\lambda \\ &= \int_{-\infty}^{+\infty} \text{Prob} \{ g(\mathbf{x}, t^*) > \mu_{\tilde{F}}^{-1}(t_0, t_0) (\Phi(x_{n+1})) \} \phi(x_{n+1}) dx_{n+1} \\ &= \int_{g(\mathbf{x}, t^*) > \mu_{\tilde{F}}^{-1}(t_0, t_0) (\Phi(x_{n+1}))} f_X(\mathbf{x}) \phi(x_{n+1}) dx dx_{n+1} \end{aligned} \tag{35}$$

The above formula transforms the time-dependent reliability under fuzzy state into a time-independent reliability with a clear safety domain $S^e = \{ (\mathbf{x}, x_{n+1}) : g(\mathbf{x}, t^*) > \mu_{\tilde{F}}^{-1}(t_0, t_0) (\Phi(x_{n+1})) \}$. Using the time-dependent generalized performance function defined by Eq. (29), the time-dependent reliability $\tilde{P}_r(t_0, t_e)$ under fuzzy state can be rewritten as the time-independent reliability with the time-independent generalized performance function $g^e(\mathbf{x}, x_{n+1})$ as follows:

$$\begin{aligned} \tilde{P}_r(t_0, t_e) &= \int_{S^e} f_X(\mathbf{x}) \phi(x_{n+1}) dx dx_{n+1} \\ &= \int_{g^e(\mathbf{x}, x_{n+1}) > 0} f_X(\mathbf{x}) \phi(x_{n+1}) dx dx_{n+1} \end{aligned} \tag{36}$$

Observing Eqs. (31) and (36), it is not difficult to find that the time-dependent reliability under fuzzy state can be solved by the traditional TIRA method under binary state. The TDFP

$\tilde{P}_f(t_0, t_e)$ under fuzzy state and the corresponding reliability $\tilde{P}_r(t_0, t_e)$ satisfy the self-duality equation $\tilde{P}_f(t_0, t_e) + \tilde{P}_r(t_0, t_e) = 1$.

2.3 SLK surrogate model method for solving TDFP under fuzzy state

The SLK surrogate model method performs well for solving the TDFP under binary state. At this time, the SLK surrogate model represents the relationship of the time-dependent performance function with respect to the random input vector and the time. In order to obtain the TDFP $\tilde{P}_f(t_0, t_e)$ under fuzzy state by using the SLK surrogate model method under binary state, it is necessary to construct the corresponding time-dependent clear generalized failure domain F_t^e corresponding to $F^e = \{ (\mathbf{x}, x_{n+1}) : g(\mathbf{x}, t^*) - \mu_{\tilde{F}}^{-1}(t_0, t_0) (\Phi(x_{n+1})) \leq 0 \}$ and the time-dependent generalized performance function $g_t^e(\mathbf{x}, x_{n+1}, t)$ corresponding to $g^e(\mathbf{x}, x_{n+1})$.

Because the first term of $g^e(\mathbf{x}, x_{n+1}) = g(\mathbf{x}, t^*) - \mu_{\tilde{F}}^{-1}(t_0, t_0) (\Phi(x_{n+1}))$ can be written as $g(\mathbf{x}, t^*) = \min_{t \in [t_0, t_e]} g(\mathbf{x}, t)$, the second term $\mu_{\tilde{F}}^{-1}(t_0, t_0) (\Phi(x_{n+1}))$ is independent of time. Therefore, the time-dependent generalized performance function $g_t^e(\mathbf{x}, x_{n+1}, t)$ corresponding to $g^e(\mathbf{x}, x_{n+1})$ and the time-dependent failure domain F_t^e corresponding to F^e can be expressed as follows:

$$g_t^e(\mathbf{x}, x_{n+1}, t) = g(\mathbf{x}, t) - \mu_{\tilde{F}}^{-1}(t_0, t_0) (\Phi(x_{n+1})) \tag{37}$$

$$F_t^e = \{ (\mathbf{x}, x_{n+1}) : g(\mathbf{x}, t) - \mu_{\tilde{F}}^{-1}(t_0, t_0) (\Phi(x_{n+1})) \leq 0, \exists t \in [t_0, t_e] \} \tag{38}$$

Equation (38) shows the equivalent time-dependent generalized clear failure domain under fuzzy state. It is not difficult to prove that the probability of F_t^e is the TDFP $\tilde{P}_f(t_0, t_e)$ under fuzzy state shown in Eq. (31). The proof is provided as follows:

$$\begin{aligned} \text{Prob} \{ F_t^e \} &= \text{Prob} \{ g(\mathbf{x}, t) - \mu_{\tilde{F}}^{-1}(t_0, t_0) (\Phi(x_{n+1})) \leq 0, \exists t \in [t_0, t_e] \} \\ &= \text{Prob} \left\{ \min_{t \in [t_0, t_e]} [g(\mathbf{x}, t) - \mu_{\tilde{F}}^{-1}(t_0, t_0) (\Phi(x_{n+1}))] \leq 0 \right\} \\ &= \text{Prob} \left\{ \min_{t \in [t_0, t_e]} g(\mathbf{x}, t) - \mu_{\tilde{F}}^{-1}(t_0, t_0) (\Phi(x_{n+1})) \leq 0 \right\} \\ &= \text{Prob} \{ g(\mathbf{x}, t^*) - \mu_{\tilde{F}}^{-1}(t_0, t_0) (\Phi(x_{n+1})) \leq 0 \} \\ &= \text{Prob} \{ g^e(\mathbf{x}, x_{n+1}) \leq 0 \} \\ &= \tilde{P}_f(t_0, t_e) \end{aligned} \tag{39}$$

Thus, it can be seen that $g_t^e(\mathbf{x}, x_{n+1}, t) = g(\mathbf{x}, t) - \mu_{\tilde{F}}^{-1}(t_0, t_0) (\Phi(x_{n+1}))$ is the time-dependent generalized performance function considering the fuzzy failure state. The SLK surrogate model method under binary state therefore can be directly

used to obtain the TDFP under fuzzy state when regarding $g_t^e(\mathbf{x}, x_{n+1}, t)$ as the time-dependent performance function. The SLK (Yun et al. 2016) is based on the cumulative confidence level, and it is demonstrated in Appendix A for the sake of conveniently reading.

3 Safety lifetime model and its solution under fuzzy state

3.1 Safety lifetime model under fuzzy state

Similar to the condition of binary state, the engineering often concerns the structural safety lifetime under the constraint of target TDFP by taking the fuzzy state into account. Taking the starting instant of service $t_0 = 0$ as an example, the safety lifetime under the constraint of target TDFP P_f^* can be obtained by the following optimization model:

$$\begin{aligned} & \text{Max } t_e \\ & \text{s.t. } \tilde{P}_f(0, t_e) \leq P_f^* \end{aligned} \tag{40}$$

where $\tilde{P}_f(0, t_e)$ is the TDFP in the working time interval $[0, t_e]$ by considering the fuzzy state.

For $t_e^{(1)} < t_e^{(2)}$, the equivalent time-dependent failure domain $F_t^e(0, t_e^{(1)})$ and $F_t^e(0, t_e^{(2)})$ corresponding to $t \in [0, t_e^{(1)}]$ and $t \in [0, t_e^{(2)}]$ are shown as follows:

$$F_t^e(0, t_e^{(1)}) = \{(\mathbf{x}, x_{n+1}) : g_t^e(\mathbf{x}, x_{n+1}, t) \leq 0, \exists t \in [0, t_e^{(1)}]\} \tag{41}$$

$$F_t^e(0, t_e^{(2)}) = \{(\mathbf{x}, x_{n+1}) : g_t^e(\mathbf{x}, x_{n+1}, t) \leq 0, \exists t \in [0, t_e^{(2)}]\} \tag{42}$$

Based on the relationship of $F_t^e(0, t_e^{(1)})$ and $F_t^e(0, t_e^{(2)})$ shown in Eq. (43), Eq. (44) holds.

$$F_t^e(0, t_e^{(1)}) \subseteq F_t^e(0, t_e^{(2)}) \tag{43}$$

$$\tilde{P}_f(0, t_e^{(1)}) = \text{Prob}\{F_t^e(0, t_e^{(1)})\} \leq \text{Prob}\{F_t^e(0, t_e^{(2)})\} = \tilde{P}_f(0, t_e^{(2)}) \tag{44}$$

Equation (44) indicates that $\tilde{P}_f(0, t_e)$ is a non-decreasing function of t_e , so the solution of the optimization model shown in Eq. (40) is the solution of the following Eq. (45):

$$\tilde{P}_f(0, t_e) = P_f^* \tag{45}$$

3.2 Solving method of safety lifetime under fuzzy state

Since the TDFP under fuzzy state $\tilde{P}_f(0, t_e)$ is a non-decreasing function of t_e , the root of Eq. (45) can be searched

efficiently by using the dichotomy. Before starting the dichotomy search, it is necessary to adaptively determine the upper bound t_u of the working time for dichotomy search, t_u should satisfy the following inequality:

$$\tilde{P}_f(0, t_u) > P_f^* \tag{46}$$

In order to determine the appropriate t_u , we can give an initial value for t_u firstly, then the SLK surrogate model method is employed to estimate $\tilde{P}_f(0, t_u)$. If $\tilde{P}_f(0, t_u) > P_f^*$ is satisfied, the Kriging surrogate model $g_{IK}^e(\mathbf{x}, x_{n+1}, t)$ established for the time-dependent generalized performance function $g_t^e(\mathbf{x}, x_{n+1}, t) = g(\mathbf{x}, t) - \mu_{\tilde{P}}^{-1}(t_0, t_0)$ ($\Phi(x_{n+1})$) in the time interval $[0, t_u]$ is used to start the dichotomy search for the safety lifetime. If t_u does not satisfy $\tilde{P}_f(0, t_u) > P_f^*$, give t_u an increment Δt_u , and let $t_u = t_u + \Delta t_u$ to adaptively search the feasible t_u continuously until $\tilde{P}_f(0, t_u) > P_f^*$, then the dichotomy search is used to find the safety lifetime. The steps for adaptively searching t_u and solving the safety lifetime t_e are shown as follows, and the corresponding flow chart is shown in Fig. 4.

Step 1 Adaptively search the feasible t_u .

Step 1.1 Set an initial value t_u as the upper bound of the search interval.

Step 1.2 Generate a $N^{\tilde{\mathbf{x}}}$ -size sample pool $S_{\tilde{\mathbf{x}}} = \{\tilde{\mathbf{x}}_1, \tilde{\mathbf{x}}_2, \dots, \tilde{\mathbf{x}}_{N^{\tilde{\mathbf{x}}}}\}$ according to the joint PDF $f_{\tilde{\mathbf{x}}}(\tilde{\mathbf{x}}) = f_{(X, X_{n+1})}(\mathbf{x}, x_{n+1}) = f_X(\mathbf{x})f_{X_{n+1}}(x_{n+1})$ of $\tilde{\mathbf{x}} = (\mathbf{x}, x_{n+1})$.

Step 1.3 Generate a N^t -size time sample pool $S_t = \{t_1, t_2, \dots, t_{N^t}\}$ based on the time interval $t \in [0, t_u]$. Then, combine $S_{\tilde{\mathbf{x}}}$ and S_t to obtain a comprehensive sample pool S as follows:

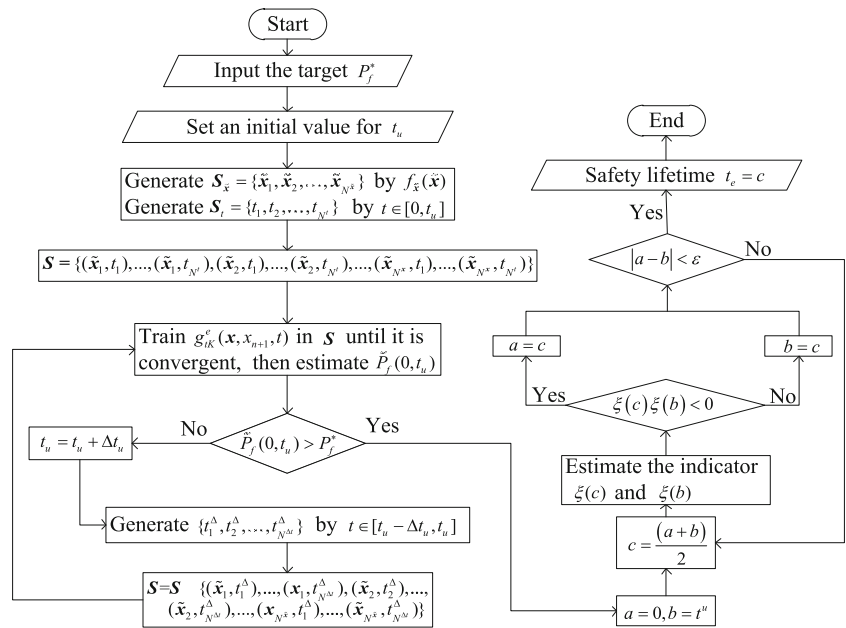
$$S = \{(\tilde{\mathbf{x}}_1, t_1), \dots, (\tilde{\mathbf{x}}_1, t_{N^t}), (\tilde{\mathbf{x}}_2, t_1), \dots, (\tilde{\mathbf{x}}_2, t_{N^t}), \dots, (\tilde{\mathbf{x}}_{N^{\tilde{\mathbf{x}}}}, t_1), \dots, (\tilde{\mathbf{x}}_{N^{\tilde{\mathbf{x}}}}, t_{N^t})\} \tag{47}$$

Step 1.4 Select the initial training set in from S and use the Kriging toolbox to establish the initial Kriging model $g_{IK}^e(\mathbf{x}, x_{n+1}, t)$ for $g_t^e(\mathbf{x}, x_{n+1}, t)$. Then, according to the learning function (Eq. (A4)) given in Appendix A, the training set and $g_{IK}^e(\mathbf{x}, x_{n+1}, t)$ are adaptively updated until $g_{IK}^e(\mathbf{x}, x_{n+1}, t)$ is converged, on which $\tilde{P}_f(0, t_u)$ is obtained accordingly.

Step 1.5 If $\tilde{P}_f(0, t_u) > P_f^*$, turn to Step 2, otherwise execute Step 1.6.

Step 1.6 Let $t_u = t_u + \Delta t_u$, generate a $N^{\Delta t}$ -size additional time sample pool $S_{\Delta t} = \{t_1^{\Delta t}, t_2^{\Delta t}, \dots, t_{N^{\Delta t}}^{\Delta t}\}$ based on $t \in [t_u - \Delta t_u, t_u]$, and a new updated sample pool S is constructed as follows.

Fig. 4 Flow chart of searching safety lifetime under fuzzy state



$$S = S \cup \{(\tilde{x}_1, t_1^\Delta), \dots, (\tilde{x}_1, t_{N^\Delta}^\Delta), (\tilde{x}_2, t_2^\Delta), \dots, (\tilde{x}_2, t_{N^\Delta}^\Delta), \dots, (\tilde{x}_{N_{\tilde{x}}}, t_1^\Delta), \dots, (\tilde{x}_{N_{\tilde{x}}}, t_{N^\Delta}^\Delta)\} \tag{48}$$

According to the learning function in Appendix A (Eq. (A4)), the training sample point is selected from S , and $g_{IK}^e(\mathbf{x}, x_{n+1}, t)$ is adaptively updated until the convergent condition is satisfied, then the $\tilde{P}_f(0, t_u)$ can be obtained accordingly. Execute Step 1.6 until $\tilde{P}_f(0, t_u) > P_f^*$.

Step 2 Search the safety lifetime t_e in the interval $[0, t_u]$ by dichotomy strategy.

Step 2.1 Set the initial value for the safety lifetime search interval $[a, b]$, let the lower bound $a = 0$, and the upper bound $b = t_u$.

Step 2.2 Set $c = (a + b)/2$.

Step 2.3 Use the $g_{IK}^e(\mathbf{x}, x_{n+1}, t)$ constructed by Step 1 to estimate $\tilde{P}_f(0, c)$, $\tilde{P}_f(0, b)$, and the corresponding indicators as follows:

$$\xi(c) = \tilde{P}_f(0, c) - P_f^* \tag{49}$$

$$\xi(b) = \tilde{P}_f(0, b) - P_f^* \tag{50}$$

Step 2.4 Update the upper and lower bounds of the safety lifetime search interval. If $\xi(b) \cdot \xi(c) > 0$, then let $b = c$, otherwise $a = c$.

Step 2.5 Determine the convergence of the dichotomy search. If $|a - b| < \epsilon$ (ϵ is the predefined precision requirement), output the safety lifetime $t_e = c$; otherwise, return to Step 2.2 and continue to search for the safety lifetime.

It can be seen from the above process that the proposed method updates the Kriging surrogate model $g_{IK}^e(\mathbf{x}, x_{n+1}, t)$ of the time-dependent generalized performance function $g_t^e(\mathbf{x}, x_{n+1}, t)$ adaptively in Step 1 for determining the feasible upper bound t_u to search the safety lifetime. Moreover, when the dichotomy search is used to search the safety lifetime after the feasible t_u is obtained, since all the time points searched in the whole dichotomy are smaller than t_u , the convergence $g_{IK}^e(\mathbf{x}, x_{n+1}, t)$ obtained from Step 1 can be used to estimate the indicator in the whole dichotomy search process, which greatly improves the efficiency for searching the safety lifetime.

4 Examples

In this section, a numerical example is employed to verify the rationality of the TDRA model under fuzzy state established in Sect. 2, and the dichotomy searching method for safety lifetime model is used in a corrosion-forced bar model under fuzzy state constrained by a target TDFP. The results obtained by the proposed method will be compared to those of the

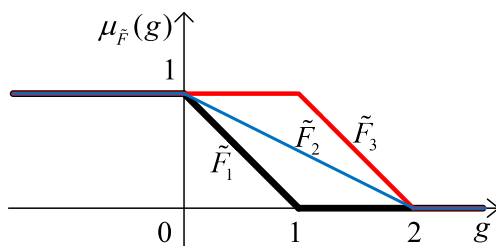


Fig. 5 Schematic diagram of $\mu_{\tilde{F}_1}(g)$, $\mu_{\tilde{F}_2}(g)$ and $\mu_{\tilde{F}_3}(g)$

Table 1 TDFP under different fuzzy failure domains and time intervals

	$t \in [0, 1]$		$t \in [0, 3]$		$t \in [0, 5]$	
	Eq. (23)	Eq. (31)	Eq. (23)	Eq. (31)	Eq. (23)	Eq. (31)
$\mu_{\tilde{F}_1}(g)$	0.02916	0.02934	0.09267	0.09268	0.14429	0.14423
$\mu_{\tilde{F}_2}(g)$	0.03201	0.03202	0.09824	0.09798	0.15033	0.15016
$\mu_{\tilde{F}_3}(g)$	0.03487	0.03490	0.10380	0.10381	0.15638	0.15637

direct Monte Carlo Simulation (D-MCS) method to verify the efficiency of the proposed method.

4.1 Verification of TDRA model under fuzzy state

Consider a numerical example with the time-dependent performance function listed as follows:

$$g(\mathbf{x}, t) = x_1 t^2 - 8x_2 t + 50(x_1 x_2 - 0.2) \tag{51}$$

$$\mu_{\tilde{F}_1}(g) = \begin{cases} 1 & g < 0 \\ 1-g & 0 \leq g \leq 1 \\ 0 & g > 1 \end{cases} \quad \mu_{\tilde{F}_2}(g) = \begin{cases} 1 & g < 0 \\ 1-\frac{g}{2} & 0 \leq g \leq 2 \\ 0 & g > 2 \end{cases} \quad \mu_{\tilde{F}_3}(g) = \begin{cases} 1 & g < 1 \\ 1-g & 1 \leq g \leq 2 \\ 0 & g > 2 \end{cases} \tag{52}$$

Figure 5 shows the schematic diagrams of the three fuzzy failure domain membership functions. In the three specific time intervals of interest $t \in [0, 1]$, $t \in [0, 3]$, and $t \in [0, 5]$, we estimate the corresponding TDFP by Eqs. (23) and (31) with 10^5 -size D-MCS, and the results are listed in Table 1. Table 2 provides the time-dependent reliability results estimated by Eqs. (32) and (36), respectively.

To illustrate the proposed method, the process of calculating the TDFP by Eq. (31) is given as follows. The first step to perform the proposed method is to introduce an auxiliary variable $X_3 \sim N(0, 1)$ (X_3 is a standard normal variable and X_3 is independent with X_1 and X_2) and establish the time-dependent generalized performance function $g_t^e(\mathbf{x}, x_3, t)$ by Eq. (37). For the example of $\mu_{\tilde{F}_1}(g)$, the $g_t^e(\mathbf{x}, x_3, t)$ is given by

$$g_t^e(\mathbf{x}, x_3, t) = x_1 t^2 - 8x_2 t + 50(x_1 x_2 - 0.2) - [1 - \Phi(x_3)] \tag{53}$$

in which the input variables X_1 and X_2 are independent normal distribution variables, and the means are $\mu_{X_1} = \mu_{X_2} = 1$, the standard deviations are $\sigma_{X_1} = \sigma_{X_2} = 0.3$.

In order to verify the rationality of the TDRA model under fuzzy state established in Sect. 2, we use Eqs. (23) and (31) and Eqs. (32) and (36) to respectively estimate the TDFP and time-dependent reliability under the following three different fuzzy failure domain membership functions.

Because X_1, X_2 , and X_3 are independent variables, the joint probability density function $f_{(X_1, X_2, X_3)}(x_1, x_2, x_3)$ of X_1, X_2 , and X_3 is given by

$$f_{(X_1, X_2, X_3)}(x_1, x_2, x_3) = f_{X_1}(x_1) \cdot f_{X_2}(x_2) \cdot f_{X_3}(x_3) \tag{54}$$

Then, the D-MCS method can be used to calculate the TDFP of Eq. (53) with $f_{(X_1, X_2, X_3)}(x_1, x_2, x_3)$ given by Eq. (54).

From Tables 1 and 2, it can be found that (1) the TDFP and the time-dependent reliability always satisfy $\tilde{P}_f(0, t_e) + \tilde{P}_r(0, t_e) = 1$, that is, $\tilde{P}_f(0, t_e)$ and $\tilde{P}_r(0, t_e)$ satisfy the self-duality property. (2) In the case of the same working time interval, the TDFPs corresponding to the fuzzy failure domains \tilde{F}_1, \tilde{F}_2 , and \tilde{F}_3 increase. It can be seen from Fig. 5 that three fuzzy failure domains satisfy $\tilde{F}_1 \subset \tilde{F}_2 \subset \tilde{F}_3$; thus the TDFP $\tilde{P}_{f_1}, \tilde{P}_{f_2}$,

Table 2 Time-dependent reliability under different fuzzy failure domains and time intervals

	$t \in [0, 1]$		$t \in [0, 3]$		$t \in [0, 5]$	
	Eq. (32)	Eq. (36)	Eq. (32)	Eq. (36)	Eq. (32)	Eq. (36)
$\mu_{\tilde{F}_1}(g)$	0.97084	0.97066	0.90733	0.90732	0.85571	0.85577
$\mu_{\tilde{F}_2}(g)$	0.96799	0.96798	0.90176	0.90202	0.84967	0.84984
$\mu_{\tilde{F}_3}(g)$	0.96513	0.96510	0.89620	0.89619	0.84362	0.84363

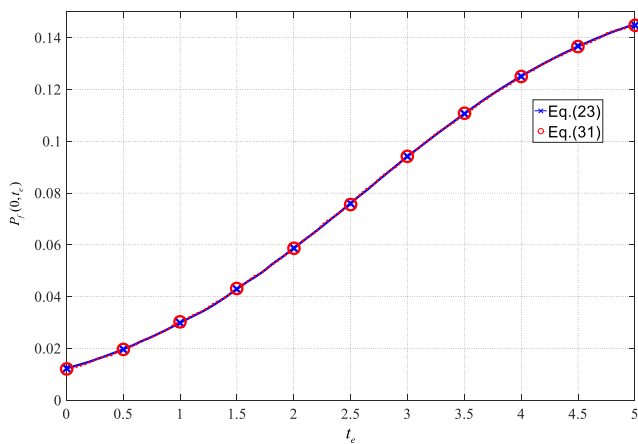


Fig. 6 Relationship curve of TDFP $P_f(0, t_e)$ vs time t_e under $\mu_{\tilde{F}_1}(g)$

and \tilde{P}_{f_3} respectively corresponding to $\tilde{F}_1, \tilde{F}_2,$ and \tilde{F}_3 should satisfy the inequality $\tilde{P}_{f_1} \leq \tilde{P}_{f_2} \leq \tilde{P}_{f_3}$, which is in agreement with the quantitative results shown in Table 1. (3) Under the same fuzzy failure domain membership function, the TDFP $\tilde{P}_f(0, t_e)$ increases with t_e , which coincides with the fact that TDFP is a non-decreasing function of the service time.

In order to further explain that the TDFP under fuzzy state obtained by Eq. (32) is a non-decreasing function with time, Fig. 6 shows the relationship curve of TDFP vs time under $\mu_{\tilde{F}_1}(g)$. It can be seen from Fig. 6 that the TDFP under fuzzy state is a non-decreasing function of the upper bound t_e of the service time interval. Combining the above three points, it is verified that the TDRA model under fuzzy state established by Eqs. (23) and (32) is reasonable.

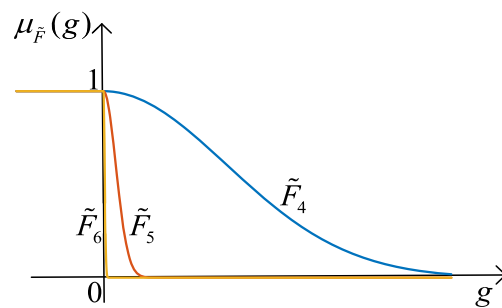


Fig. 7 Schematic diagram of $\mu_{\tilde{F}_4}(g), \mu_{\tilde{F}_5}(g),$ and $\mu_{\tilde{F}_6}(g)$

Continue to observe Table 1, it can be seen that in the case where the fuzzy failure domain membership function and the time observation interval are the same, the result obtained by Eq. (23) is consistent with that obtained by Eq. (31), which is also confirmed by Fig. 6. It can also be seen in Table 2 that the time-dependent reliability results under fuzzy state estimated by Eqs. (32) and (36) are also consistent, which fully demonstrates the rationality and correctness of the generalized performance function under binary state $g^e(x, x_{n+1})$ obtained by introducing an auxiliary variable based on Eq. (23). To further illustrate that Eqs. (23) and (31) are still consistent under different forms of fuzzy failure domain membership function, Table 3 shows the TDFP results under the Gaussian fuzzy failure domain membership function $\mu_{\tilde{F}_4}(g), \mu_{\tilde{F}_5}(g),$ and $\mu_{\tilde{F}_6}(g)$ in the time observation interval $t \in [0, 5]$. The formulas of $\mu_{\tilde{F}_4}(g), \mu_{\tilde{F}_5}(g),$ and $\mu_{\tilde{F}_6}(g)$ are shown as follows. Figure 7 shows the schematic diagram of these three kinds of fuzzy failure domain membership functions.

$$\mu_{\tilde{F}_4}(g) = \begin{cases} 1 & g < 0 \\ \exp\left(-\frac{g^2}{100}\right) & g \geq 0 \end{cases} \quad \mu_{\tilde{F}_5}(g) = \begin{cases} 1 & g < 0 \\ \exp(-g^2) & g \geq 0 \end{cases} \quad \mu_{\tilde{F}_6}(g) = \begin{cases} 1 & g < 0 \\ \exp(-100g^2) & g \geq 0 \end{cases} \quad (55)$$

It can be seen from Table 3 that the results obtained by Eqs. (23) and (31) are still consistent under Gaussian fuzzy failure domain membership function. At the same time, it can be seen from Fig. 7 that $\tilde{F}_4 \supset \tilde{F}_5 \supset \tilde{F}_6$. Therefore, the TDFP $\tilde{P}_{f_4}, \tilde{P}_{f_5},$ and \tilde{P}_{f_6} respectively corresponding to $\tilde{F}_4, \tilde{F}_5,$ and \tilde{F}_6 should

satisfy $\tilde{P}_{f_4} \geq \tilde{P}_{f_5} \geq \tilde{P}_{f_6}$, which is consistent with the quantitative results shown in Table 3.

In order to validate that the proposed method is applicable to the non-normal inputs, Table 5 gives the TDFP obtained by Eqs. (23) and (31) in the case of $\mu_{\tilde{F}_1}(g)$ and $t \in [0, 5]$ where the input variables obey different non-normal distributions shown in Table 4.

From Table 5, we can see that the TDFP obtained by Eqs. (23) and (31) are still applicable to the different non-normal distributions of the input variables, which means that the proposed method has no limit for the distribution type of the inputs.

Table 3 TDFP under different fuzzy failure domains

	$\mu_{\tilde{F}_4}(g)$	$\mu_{\tilde{F}_5}(g)$	$\mu_{\tilde{F}_6}(g)$
Eq. (23)	0.27207	0.14892	0.13982
Eq. (31)	0.27233	0.14898	0.13983

Table 4 Distributions and corresponding parameters of X_1 and X_2

	X_1			X_2		
	Parameter 1	Parameter 2	Distribution type	Parameter 1	Parameter 2	Distribution type
Case 1	$\mu = 0.6$	$\sigma = 0.3$	Lognormal	$\mu = 1$	$\sigma = 0.3$	Lognormal
Case 2	$Low = 0.5$	$Up = 1.5$	Uniform	$Low = 0.5$	$Up = 1.5$	Uniform
Case 3	$\mu = 1$	$\sigma = 0.3$	Extreme I	$\mu = 1$	$\sigma = 0.3$	Extreme I

μ mean, σ standard deviation, Low lower boundary, Up upper boundary

Through the above analysis, the rationality of the TDRA model under fuzzy state established in Sect. 2 is fully verified, and it is completely reasonable and feasible to convert the TDRA model under fuzzy state into that with binary state by adding an auxiliary variable.

4.2 Corrosion-forced bar model

Figure 8 is a schematic diagram of a corrosion-forced bar (Sudret 2008) whose random input vector in the time-dependent performance function is $X = \{a_0, b_0, \sigma_u, F\}$, where a_0 is the initial length of vertical section of the bar, and b_0 is the initial height; σ_u is the ultimate stress of the material, and F is the force applied to the midpoint of the bar. All input

variables obey the normal distribution, and their parameters are shown in Table 6.

Now consider the influence of corrosion on the structure, and assume that the width a and height b of the bar section have the following relationship with the corrosion time t :

$$a(t) = a_0 - 2\kappa t, \quad b(t) = b_0 - 2\kappa t \tag{56}$$

in which the corrosion coefficient $\kappa = 0.25\text{mm/year}$.

The law of the external load subjected to the midpoint of the bar is $\sin(t/4)F$, which changes with time. According to these conditions, the time-dependent performance function of the corrosion-forced bar can be established as follows:

$$G(X, t) = \frac{M_u(t) - M(t)}{1000} = \left[\frac{a(t)b^2(t)\sigma_u}{4} - \left(\frac{\sin(t/4)FL}{4} + \frac{\rho_{st}a_0b_0L^2}{8} \right) \right] \times \frac{1}{1000} \tag{57}$$

in which $M_u(t) = \frac{a(t)b^2(t)\sigma_u}{4}$ is the ultimate bending moment of the bar, $M(t) = \frac{FL}{4} + \frac{\rho_{st}a_0b_0L^2}{8}$ is the bending moment at the midpoint of the bar, and it is the largest bending moment. ρ_{st} indicates the density of the bar, and $\rho_{st} = 78.5\text{kN/m}^3$. L is the length of the bar, and $L = 9\text{m}$.

For this example, the safety lifetime is obtained by the method shown in Sect. 3 under the fuzzy states with membership functions $\mu_{\tilde{F}_1}(g)$, $\mu_{\tilde{F}_2}(g)$, and $\mu_{\tilde{F}_3}(g)$ in Eq. (52), and the corresponding target TDFP $P_f^* = 0.01$, the accuracy requirement is set as $\varepsilon = 0.001$. Table 7 gives comparison of the safety lifetime results under different fuzzy failure domains.

In Table 7, t_e is the estimated safety lifetime, and N_{call} indicates the number of calling the time-dependent performance function. Because $\tilde{F}_1 \subset \tilde{F}_2 \subset \tilde{F}_3$, the safety lifetimes t_{e1} , t_{e2} , and t_{e3} corresponding to \tilde{F}_1 , \tilde{F}_2 , and \tilde{F}_3 respectively

should qualitatively satisfy $t_{e1} \geq t_{e2} \geq t_{e3}$, which is consistent with the quantitative results shown in Table 7. Since the dichotomy search only requires to call the established Kriging model constructed in the first step for searching the feasible t_u , the safety lifetime can be efficiently estimated by the SLK surrogate model. In the other hand, the D-MCS method needs to call the actual time-dependent performance function in each step of dichotomy search; thus, the computational burden of the D-MCS is very heavy. It can be seen from Table 7 that the results obtained by the SLK surrogate model method are consistent with those by the D-MCS method, which verifies the correctness of the SLK surrogate model method. To further illustrate the correctness of the SLK method, Fig. 9 shows the relationship curves of $P_f(0, t_e)$ vs t_e (the upper bound of the working time interval $[0, t_e]$) under the fuzzy failure domain

Table 5 TDFP under different cases

	Case 1	Case 2	Case 3
Eq. (23)	0.00125	0.17220	0.33924
Eq. (31)	0.00126	0.17220	0.33931

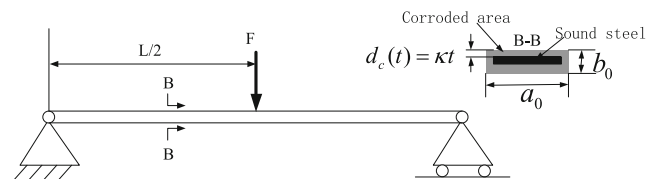


Fig. 8 Corrosion-forced bar model (Sudret 2008)

Table 6 Distribution types and parameters of input variables of corrosion-forced bar

Variables	Distribution type	Mean	Standard deviation
$a_0(\text{m})$	Normal	0.2	0.01
$b_0(\text{m})$	Normal	0.04	0.001
$\sigma_u(\text{Pa})$	Normal	2.4×10^8	1×10^7
$F(N)$	Normal	3500	100

Table 7 Safety lifetime under different fuzzy failure domains

	Single-loop Kriging		Direct MCS	
	t_e	N_{call}	t_e	N_{call}
$\mu_{\tilde{F}_1}(\mathbf{g})$	4.761	106	4.760	4×10^8
$\mu_{\tilde{F}_2}(\mathbf{g})$	4.190	112	4.190	4×10^8
$\mu_{\tilde{F}_3}(\mathbf{g})$	4.011	127	4.011	4×10^8

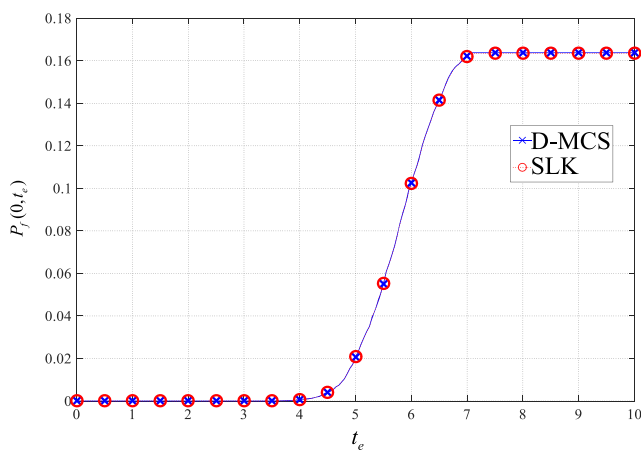


Fig. 9 $P_f(0, t_e)$ vs t_e under \tilde{F}_1

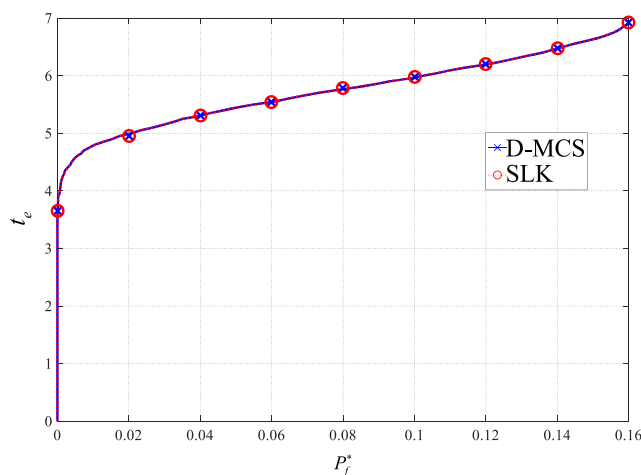


Fig. 10 Safety lifetime t_e vs P_f^*

\tilde{F}_1 estimated respectively by the SLK method and the D-MCS method, while Fig. 10 shows the curve of the safety lifetime t_e vs target TDFP P_f^* .

It can be seen from Fig. 9 that the TDFP $P_f(0, t_e)$ obtained by the SLK method is almost identical to that by the D-MCS method, and the TDFP under fuzzy state increases with t_e . From Fig. 10, we can see that the safety lifetime obtained by the SLK method is also completely consistent with that by the D-MCS method, and the safety lifetime is increased with P_f^* increasing. These results fully illustrate that the SLK surrogate model method is efficient and accurate in analyzing the safety lifetime under fuzzy state.

5 Conclusion

The main contribution of this paper is to establish a TDRA model under fuzzy state and construct a safety lifetime model based on the target TDFP constraint. In the process of establishing the TDRA model under fuzzy state, the TDRA model under binary state is firstly transformed. The TDFP under binary state is expressed in the form of time-dependent failure domain indicator function; then based on the basic principle of establishing the TIRA model under fuzzy state, the TDRA model under fuzzy state is reasonably derived. After that, the auxiliary variable and time-dependent generalized performance function are introduced to simplify the established TDRA model under fuzzy state. Based on the obtained TDRA model, the safety lifetime model under fuzzy state is established, and the SLK surrogate model method is employed to estimate the TDFP and solve the safety lifetime under fuzzy state. Through the qualitative and quantitative comparison analysis of the examples, the correctness and rationality of the TDRA model under fuzzy state established in this paper are fully verified. The correctness and efficiency of using the SLK surrogate model method to estimate the TDFP and the safety lifetime under fuzzy state are also verified.

At the same time, it should be noted that the TDRA model under fuzzy state established in this paper is based on the assumption that the membership function of fuzzy failure domain does not change with time. How to establish the TDRA model under fuzzy state in which the membership function of fuzzy failure domain changes with time will be carried out in the subsequent work.

6 Replication of results

The MATLAB code of searching the safety lifetime for example 4.2 is presented as follows, where the “dace” toolbox is utilized for constructing the SLK model. When the performance function “G” needs to be estimated, the function “G1” is called.

Funding information This work was supported by the National Natural Science Foundation of China (Grant 51775439) and the National Science and Technology Major Project (2017-IV-0009-0046).

Compliance with ethical standards

Conflict of interest The authors declare that they have no conflict of interest.

Appendix A. SLK surrogate model method

The SLK surrogate model method used in this paper adopts the idea of single-loop adaptive sampling meta-model method in ref. Yun et al. (2016). The main feature of this method is the introduction of new convergence criteria and update point selection criteria. The convergence criteria is that the cumulative confidence level C is greater than a predefined confidence target C^* (0.9999 is used in this paper, and the larger C^* corresponds the more accurate results). C is determined by the following formula:

$$C = E(\text{Pr}_c) = \frac{1}{N} \sum_{i=1}^N \left(\frac{1}{N_t} \sum_{j=1}^{N_t} \text{Pr}_c(\mathbf{x}_i, t_j) \right) \tag{A1}$$

in which $E(\cdot)$ is expectation operator, N is the number of samples extracted by the PDF of \mathbf{x} , N_t is the number of time-discrete points uniformly extracted in the time interval, and $\text{Pr}_c(\mathbf{x}_i, t_j)$ indicates the probability of correctly identifying the sign of the response at the sample point \mathbf{x}_i and time instant t_j by the built Kriging model, which is determined by the following formula (Echard et al. 2011):

$$\text{Pr}_c(\mathbf{x}_i, t_j) = \Phi \left(\frac{|g_K(\mathbf{x}_i, t_j)|}{\sigma_{g_K}(\mathbf{x}_i, t_j)} \right) \tag{A2}$$

in which $\Phi(\cdot)$ is the cumulative distribution function of the standard normal distribution, $g_K(\cdot)$ represents the predicted value of the Kriging model, and $\sigma_{g_K}(\cdot)$ represents the standard deviation of the predicted value.

In order to maximize the cumulative confidence level, the following criteria is used (Wang and Wang 2013):

$$\psi(\mathbf{x}_i, t_j) = (1 - \text{Pr}_c(\mathbf{x}_i, t_j)) \times f_{(\mathbf{x},t)}(\mathbf{x}_i, t_j) \times \sigma_{g_K}(\mathbf{x}_i, t_j) \tag{A3}$$

where $f_{(\mathbf{x},t)}(\mathbf{x}_i, t_j)$ is the PDF of the point (\mathbf{x}_i, t_j) .

In order to maximize the confidence level of the Kriging model, the point that maximizes the contribution to the cumulative confidence level should be added to update the Kriging model, i.e., update point is selected by the following Eq. (A4).

$$(\mathbf{x}_i, t_j) = \arg \max_{i,j} \psi(\mathbf{x}_i, t_j) \quad i = 1, 2, \dots, N \quad j = 1, 2, \dots, N_t \tag{A4}$$

By using the convergence criteria $C > C^*$ and update point selection criteria shown in Eq. (A4), the established Kriging model can have a higher cumulative confidence level in the global scope, on which the reliability analysis result can be more accurate. For the time-dependent generalized performance function considering fuzzy state shown in Eq. (37), the steps for solving the TDFP are listed as follows:

Step 1 Generate a $N_{\tilde{\mathbf{x}}}$ -size sample pool $\mathcal{S}_{\tilde{\mathbf{x}}} = \{\tilde{\mathbf{x}}_1, \tilde{\mathbf{x}}_2, \dots, \tilde{\mathbf{x}}_{N_{\tilde{\mathbf{x}}}}\}$ by $f_{\tilde{\mathbf{x}}}(\tilde{\mathbf{x}})$.

Step 2 Generate an N_t -size time sample pool $S_t = \{t_1, t_2, \dots, t_{N_t}\}$ based on $t \in [t_0, t_e]$, then combine $\mathcal{S}_{\tilde{\mathbf{x}}}$ and S_t to obtain the comprehensive sample pool shown as follows:

$$\mathcal{S} = \left\{ (\tilde{\mathbf{x}}_1, t_1), \dots, (\tilde{\mathbf{x}}_1, t_{N_t}), (\tilde{\mathbf{x}}_2, t_1), \dots, (\tilde{\mathbf{x}}_2, t_{N_t}), \dots, (\tilde{\mathbf{x}}_{N_{\tilde{\mathbf{x}}}}, t_1), \dots, (\tilde{\mathbf{x}}_{N_{\tilde{\mathbf{x}}}}, t_{N_t}) \right\} \tag{A5}$$

Step 3 Select the initial training set from \mathcal{S} , and use the Kriging toolbox to establish the initial surrogate model $g_{iK}^e(\mathbf{x}, x_{n+1}, t)$ of the $g_t^e(\mathbf{x}, x_{n+1}, t)$ in \mathcal{S} .

Step 4 Calculate the cumulative confidence level C according to Eq. (A1) to determine whether $C > C^*$ is satisfied, if $C > C^*$, execute to Step 5. Otherwise, select the update point by Eq. (A4) and add it in the training set to update $g_{iK}^e(\mathbf{x}, x_{n+1}, t)$ until $C > C^*$.

Step 5 Estimate $\tilde{P}_f(t_0, t_e)$ by

$$\tilde{P}_f(t_0, t_e) = \frac{N_f}{N_{\tilde{\mathbf{x}}}} \tag{A6}$$

where N_f is the number of failure sample points screened by $g_{iK}^e(\mathbf{x}, x_{n+1}, t)$ in \mathcal{S} .

```

clear all
clc
G=@(x)G1(x)-(1-normcdf(x(:,5)));
Pfx=0.01;
tll=10;
mu=[0.2,0.04,2.4e8,3500,0,0];
sigma=[0.01,0.001,1e7,100,1,tll];
pdfg=@(x)normpdf(x(:,1),mu(1),sigma(1)).*normpdf(x(:,2),mu(2),sigma(2))
).*normpdf(x(:,3),mu(3),...

sigma(3)).*normpdf(x(:,4),mu(4),sigma(4)).*normpdf(x(:,5),mu(5),sigma
(5)).*unifpdf(x(:,6),mu(6),sigma(6));
vn=length(mu);
p=sobolset(2.*vn,'Skip',5e4);
N1=10;           %size of initial sample
N3=1e4;         %size of sample pool
N4=1e2;         %size of time pool
P=p(1:N1,1:vn); %initial sample pool
PP=p(1:N3,vn+1:2*vn);
X=zeros(N3,vn-1); %sample pool
t=zeros(N4,1);  %time pool
for i=1:vn
    if i<=vn-1
        P(:,i)=norminv(P(:,i),mu(i),sigma(i));
        X(:,i)=norminv(PP(:,i),mu(i),sigma(i));
    else
        P(:,i)=unifinv(P(:,i),mu(i),sigma(i));
        t(:,1)=unifinv(PP(1:N4,i),mu(i),sigma(i));
    end
end
end
t=sort(t);
PMC=zeros(N3*N4,vn);
for i=1:N3
    PMC((i-1)*N4+1:(i-1)*N4+N4,:)=[ones(N4,1)*X(i,:),t];
end
save all

%% Establish the Kriging model
% load all
for i=1:N1

```

```

        yp(i)=G(P(i,:));
    end
    yP=yp';
    theta=ones(1,vn).*0.01;
    lob=ones(1,vn).*1e-5;
    upb=ones(1,vn).*20;
    for i=1:1000
        eit=zeros(N3*N4,1);
        prxi=zeros(N3*N4,1);
        if i==1
            x=P;
            y=yP;
            dmodel=dacefit(x,y,@regpoly0,@corrgauss,theta,lob,upb);
            [ug,sigmag]=predictor(PMC,dmodel);

            eit=(1-normcdf((abs(ug))./sqrt(sigmag))).*sqrt(sigmag).*pdfg(PMC);
            prxi=normcdf((abs(ug))./sqrt(sigmag));
            [~,I]=max(eit);
        else
            x(N1-1+i,:)=PMC(I,:);
            y(N1-1+i)=G(PMC(I,:));
            dmodel=dacefit(x,y,@regpoly0,@corrgauss,theta,lob,upb);
            ug=ones(N3*N4,1);
            sigma=ones(N3*N4,1);
            for ii=1:N4

                [ug((ii-1)*N3+1:ii*N3,1),sigmag((ii-1)*N3+1:ii*N3,1)]=predictor(PMC((
                ii-1)*N3+1:ii*N3,:),dmodel);
            end

            eit=(1-normcdf((abs(ug))./sqrt(sigmag))).*sqrt(sigmag).*pdfg(PMC);
            prxi=normcdf((abs(ug))./sqrt(sigmag));
            [~,I]=max(eit);
        end
        Cr(i)=mean(prxi);
        fprintf('i=%d,Cr=%.6f\n',i,Cr(i));
        if Cr(i)>0.9999
            break
        end
    end
    fprintf('SLK has been established!!!!');
    save all

```



```

%% Searching safety lifetime by dichotomy search
% load all
a=0;b=t11;          % D-MCS
while abs(a-b)>0.001
    S=X;
    t11=(a+b)/2;
    if t11==0
        tt=zeros(N4,1);
    else
        tt=unifinv(PP(1:N4,vn),0,t11);
    end
    for i=1:N4
        n=size(S);
        B=[S,ones(n(1),1)*tt(i)];
        yb1=G(B);
        [I,~]=find(yb1<0);
        S(I,:)=[];
    end
    n=size(S);
    c=1-n(1)/(N3)-Pfx;
    if c<0
        a=t11;
    else
        b=t11;
    end
end
save('smMCS.txt','t11','-append','-ascii');

a=0;b=t11;          %SLK
while abs(a-b)>0.001
    S=X;
    t1=(a+b)/2;
    if t1==0
        tt=zeros(N4,1);
    else
        tt=unifinv(PP(1:N4,vn),0,t1);
    end
    for i=1:N4
        n=size(S);
        B=[S,ones(n(1),1)*tt(i)];
        yb1=predictor(B,dmodel);
        [I,~]=find(yb1<0);
        S(I,:)=[];
    end
end

```

```

n=size(S);
c=1-n(1)/(N3)-Pfx;
if c<0
    a=t1;
else
    b=t1;
end
end
save('smKRG.txt','t1','-append','-ascii');
save all

function [ y ] = G1( x )
%time-dependent performance function
a=x(:,1)-0.0005*x(:,6);
b=x(:,2)-0.0005*x(:,6);
Mu=a.*b.^2.*x(:,3)/4;
M=sin(x(:,6)/4).*x(:,4)*9/4+78500.*x(:,1).*x(:,2)*81/8;
G=Mu-M;
y=G/1000
end

```

References

- Andrieu-Renaud C, Sudret B, Lemaire M (2004) The PHI2 method: a way to compute time-variant reliability. *Reliab Eng Syst Saf* 84:75–86. <https://doi.org/10.1016/j.res.2003.10.005>
- Au SK (2004) Probabilistic failure analysis by importance sampling Markov chain simulation. *J Eng Mech* 130:303–311. [https://doi.org/10.1061/\(ASCE\)0733-9399\(2004\)130:3\(303\)](https://doi.org/10.1061/(ASCE)0733-9399(2004)130:3(303))
- Au SK, Beck JL (1999) A new adaptive importance sampling scheme for reliability calculations. *Struct Saf* 21:135–158. [https://doi.org/10.1016/S0167-4730\(99\)00014-4](https://doi.org/10.1016/S0167-4730(99)00014-4)
- Au SK, Beck JL (2001) Estimation of small failure probabilities in high dimensions by subset simulation. *Probab Eng Mech* 16:263–277. [https://doi.org/10.1016/s0266-8920\(01\)00019-4](https://doi.org/10.1016/s0266-8920(01)00019-4)
- Baran I, Tutum CC, Hattel JH (2012) Reliability estimation of the pultrusion process using the first-order reliability method (FORM). *Appl Compos Mater* 20:639–653. <https://doi.org/10.1007/s10443-012-9293-4>
- Cai KY, Wen CY, Zhang ML (1991a) Fuzzy reliability modeling of gracefully degradable computing systems. *Reliab Eng Syst Saf* 33:141–157. [https://doi.org/10.1016/0951-8320\(91\)90030-B](https://doi.org/10.1016/0951-8320(91)90030-B)
- Cai KY, Wen CY, Zhang ML (1991b) Fuzzy variables as a basis for a theory of fuzzy reliability in the possibility context. *Fuzzy Sets Syst* 42:145–172. [https://doi.org/10.1016/0165-0114\(91\)90143-E](https://doi.org/10.1016/0165-0114(91)90143-E)
- Cai KY, Wen CY, Zhang ML (1993) Fuzzy states as a basis for a theory of fuzzy reliability. *Microelectron Reliab* 33:2253–2263. [https://doi.org/10.1016/0026-2714\(93\)90065-7](https://doi.org/10.1016/0026-2714(93)90065-7)
- Chen L, Lu ZZ (2007) A new numerical method for general failure probability with fuzzy failure region. *Key Eng Mater* 353-358:997–1000. <https://doi.org/10.4028/www.scientific.net/KEM.353-358.997>
- Cheng K, Lu ZZ (2018a) Adaptive sparse polynomial chaos expansions for global sensitivity analysis based on support vector regression. *Comput Struct* 194:86–96. <https://doi.org/10.1016/j.compstruc.2017.09.002>
- Cheng K, Lu ZZ (2018b) Sparse polynomial chaos expansion based on D-MORPH regression. *Appl Math Comput* 323:17–30 <https://doi.org/10.1016/j.amc.2017.11.044>
- Ditlevsen O, Melchers RE, Gluwer H (1990) General multi-dimensional probability integration by directional simulation. *Comput Struct* 36:355–368. [https://doi.org/10.1016/0045-7949\(90\)90134-N](https://doi.org/10.1016/0045-7949(90)90134-N)
- Du XP (2014) Time-dependent mechanism reliability analysis with envelope functions and first-order approximation. *J Mech Des* 136:081010–0811-7. <https://doi.org/10.1115/1.4027636>
- Echard B, Gayton N, Lemaire M (2011) AK-MCS: an active learning reliability method combining kriging and Monte Carlo simulation. *Struct Saf* 33:145–154. <https://doi.org/10.1016/j.strusafe.2011.01.002>
- Fan CQ, Lu ZZ, Shi Y (2018) Safety life analysis under the required failure possibility constraint for structure involving fuzzy uncertainty. *Struct Multidiscip Optim* 58:287–303. <https://doi.org/10.1007/s00158-017-1896-9>
- Feng KX, Lu ZZ, Pang C, Yun WY (2018) Efficient numerical algorithm of profust reliability analysis: an application to wing box structure. *Aerosp Sci Technol* 80:203–211. <https://doi.org/10.1016/j.ast.2018.07.009>

- Feng KX, Lu ZZ, Ling CY, Yun WY (2019) Efficient computational method based on AK-MCS and Bayes formula for time-dependent failure probability function. *Struct Multidiscip Optim*. <https://doi.org/10.1007/s00158-019-02265-z>
- Grooteman F (2008) Adaptive radial-based importance sampling method for structural reliability. *Struct Saf* 30:533–542. <https://doi.org/10.1016/j.strusafe.2007.10.002>
- Hu Z, Du XP (2013) Time-dependent reliability analysis with joint upcrossing rates. *Struct Multidiscip Optim* 48:893–907. <https://doi.org/10.1007/s00158-013-0937-2>
- Hu Z, Mahadevan S (2016) A single-loop kriging surrogate modeling for time-dependent reliability analysis. *J Mech Des* 138:061406–061-10. <https://doi.org/10.1115/1.4033428>
- Hu Z, Li HF, Du XP, Chandrashekhara K (2013) Simulation-based time-dependent reliability analysis for composite hydrokinetic turbine blades. *Struct Multidiscip Optim* 47:765–781. <https://doi.org/10.1007/s00158-012-0839-8>
- Li J, Chen JB, Fan WL (2007) The equivalent extreme-value event and evaluation of the structural system reliability. *Struct Saf* 29:112–131. <https://doi.org/10.1016/j.strusafe.2006.03.002>
- Onisawa T (1990) An application of fuzzy concepts to modelling of reliability analysis. *Fuzzy Sets Syst* 37:267–286. [https://doi.org/10.1016/0165-0114\(90\)90026-3](https://doi.org/10.1016/0165-0114(90)90026-3)
- Sahinidis NV (2004) Optimization under uncertainty: state-of-the-art and opportunities. *Comput Chem Eng* 28:971–983. <https://doi.org/10.1016/j.compchemeng.2003.09.017>
- Schuëller GI, Pradlwarter HJ, Koutsourelakis PS (2004) A critical appraisal of reliability estimation procedures for high dimensions. *Probab Eng Mech* 19:463–474. <https://doi.org/10.1016/j.probabeng.2004.05.004>
- Shi Y, Lu ZZ, Cheng K, Zhou YC (2017a) Temporal and spatial multi-parameter dynamic reliability and global reliability sensitivity analysis based on the extreme value moments. *Struct Multidiscip Optim* 56:117–129. <https://doi.org/10.1007/s00158-017-1651-2>
- Shi Y, Lu ZZ, Zhang KC, Wei YH (2017b) Reliability analysis for structures with multiple temporal and spatial parameters based on the effective first-crossing point. *J Mech Des* 139:121403–1211-9. <https://doi.org/10.1115/1.4037673>
- Shi Y, Lu ZZ, Chen SY, Xu LY (2018a) A reliability analysis method based on analytical expressions of the first four moments of the surrogate model of the performance function. *Mech Syst Signal Process* 111:47–67. <https://doi.org/10.1016/j.ymsp.2018.03.060>
- Shi Y, Lu ZZ, Zhou YC (2018b) Time-dependent safety and sensitivity analysis for structure involving both random and fuzzy inputs. *Struct Multidiscip Optim* 58:2655–2675. <https://doi.org/10.1007/s00158-018-2043-y>
- Song SF, Lu ZZ (2007) Improved line sampling reliability analysis method and its application. *Key Eng Mater* 353-358:1001–1004. <https://doi.org/10.4028/www.scientific.net/KEM.353-358.1001>
- Song SF, Lu ZZ, Qiao HW (2009) Subset simulation for structural reliability sensitivity analysis. *Reliab Eng Syst Saf* 94:658–665. <https://doi.org/10.1016/j.res.2008.07.006>
- Sudret B (2008) Analytical derivation of the outcrossing rate in time-variant reliability problems. *Struct Infrastruct Eng* 4:353–362. <https://doi.org/10.1080/15732470701270058>
- Tang ZC, Lu ZZ (2014) Reliability-based design optimization for the structures with fuzzy variables and uncertain-but-bounded variables. *J Aerosp Inform Syst* 11:412–422. <https://doi.org/10.2514/1.1010140>
- Wang ZQ, Wang PF (2013) A maximum confidence enhancement based sequential sampling scheme for simulation-based design. *J Mech Des* 136:021006–021010. <https://doi.org/10.1115/1.4026033>
- Wang ZQ, Wang PF (2015) A double-loop adaptive sampling approach for sensitivity-free dynamic reliability analysis. *Reliab Eng Syst Saf* 142:346–356. <https://doi.org/10.1016/j.res.2015.05.007>
- Wang JQ, Lu ZZ, Shi Y (2018a) Aircraft icing safety analysis method in presence of fuzzy inputs and fuzzy state. *Aerosp Sci Technol* 82-83: 172–184. <https://doi.org/10.1016/j.ast.2018.09.003>
- Wang ZL, Cheng XW, Liu J (2018b) Time-dependent concurrent reliability-based design optimization integrating experiment-based model validation. *Struct Multidiscip Optim* 57:1523–1531. <https://doi.org/10.1007/s00158-017-1823-0>
- Wang ZH, Wang ZL, Yu S, Zhang KW (2019) Time-dependent mechanism reliability analysis based on envelope function and vine-copula function. *Mech Mach Theory* 134:667–684. <https://doi.org/10.1016/j.mechmachtheory.2019.01.008>
- Yang XF, Mi CY, Deng DY, Liu YS (2019) A system reliability analysis method combining active learning kriging model with adaptive size of candidate points. *Struct Multidiscip Optim*. <https://doi.org/10.1007/s00158-019-02205-x>
- Yu S, Wang ZL (2018) A novel time-variant reliability analysis method based on failure processes decomposition for dynamic uncertain structures. *J Mech Des* 140:051401–051411. <https://doi.org/10.1115/1.4039387>
- Yu S, Wang ZL, Zhang KW (2018) Sequential time-dependent reliability analysis for the lower extremity exoskeleton under uncertainty. *Reliab Eng Syst Saf* 170:45–52. <https://doi.org/10.1016/j.res.2017.10.006>
- Yun WY, Lu ZZ, Jiang X, Zhao LF (2016) Maximum probable life time analysis under the required time-dependent failure probability constraint and its meta-model estimation. *Struct Multidiscip Optim* 55: 1439–1451. <https://doi.org/10.1007/s00158-016-1594-z>

Publisher's note Springer Nature remains neutral with regard to jurisdictional claims in published maps and institutional affiliations.